S.T. Yau High School Science Award

Research Report

Name of team member: Hanna Hong
School: Riverside High School
City, Country: Leesburg, Virginia

Name of supervising teacher: Ji-Hoon Lee
Job Title: Research Intern
School/Institution: Luminescent MD, Inc.
City, Country: Maryland

Rapid Aβ42 Quantification Using a Wash-Free Chemiluminescent Aptasensor toward Alzheimer's Disease Diagnosis

September 12th, 2026

Rapid Aβ42 Quantification Using a Wash-Free Chemiluminescent Aptasensor toward Alzheimer's Disease Diagnosis

Hanna E. Hong

Abstract

A wash-free graphene oxide (GO)-based aptasensor with acridinium ester chemiluminescence detection was developed for the rapid quantification of amyloid-β1–42 (Aβ42). An amine-modified Aβ42 aptamer was conjugated with acridinium ester–NHS and temporarily immobilized on a GO film-coated well through noncovalent interactions. Aβ42 binding induced a conformational change in the aptamer that weakened its interaction with GO and released the Aβ42–aptamer–AE complex into solution. The released complex was directly transferred for chemiluminescence detection without a washing step during sample analysis. Under the optimized conditions, the aptasensor quantified Aβ42 over 78.5–5,000 pg/mL, with a limit of detection of 27 pg/mL and a lower limit of quantification of 78.5 pg/mL. The total analytical reaction and detection time was approximately 31 minutes. Recovery from artificial cerebrospinal fluid ranged from 92.3% to 112.7%, with a mean recovery of 104.6%. The coefficients of variation ranged from 4.2% to 6.9% for triplicate measurements, demonstrating acceptable preliminary accuracy and precision. Aβ40 (100 ng/mL) and total tau (2,500 pg/mL), tested at concentrations exceeding their typical CSF ranges, and human serum albumin (0.2 mg/mL) produced signals comparable to the buffer blank, whereas Aβ42 generated an approximately 2.4-fold higher response. These findings support the analytical selectivity and feasibility of the wash-free GO-based aptasensor for sensitive Aβ42 quantification. Further validation using human cerebrospinal fluid and direct comparison with automated clinical systems are required to establish its clinical utility as a potential tool for the diagnosis of Alzheimer's disease.

Keywords: amyloid-β1–42; Aβ42 aptamer; wash-free aptasensor; graphene oxide film; acridinium ester chemiluminescence; cerebrospinal fluid; Alzheimer's disease

Acknowledgement

I sincerely thank Luminescent MD, Inc. for providing me with this research internship opportunity. I am especially grateful to Dr. Lee for his support and mentorship throughout the process of collecting my data and preparing this manuscript.

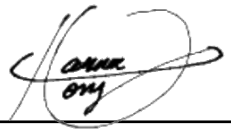
Commitments on Academic Honesty and Integrity

We hereby declare that we

1. are fully committed to the principle of honesty, integrity and fair play throughout the competition.
2. actually perform the research work ourselves and thus truly understand the content of the work.
3. observe the common standard of academic integrity adopted by most journals and degree theses.
4. have declared all the assistance and contribution we have received from any personnel, agency, institution, etc. for the research work.
5. undertake to avoid getting in touch with assessment panel members in a way that may lead to direct or indirect conflict of interest.
6. undertake to avoid any interaction with assessment panel members that would undermine the neutrality of the panel member and fairness of the assessment process.
7. observe the safety regulations of the laboratory(ies) where we conduct the experiment(s), if applicable.
8. observe all rules and regulations of the competition.
9. agree that the decision of YHSA is final in all matters related to the competition.

We understand and agree that failure to honour the above commitments may lead to disqualification from the competition and/or removal of reward, if applicable; that any unethical deeds, if found, will be disclosed to the school principal of team member(s) and relevant parties if deemed necessary; and that the decision of YHSA is final and no appeal will be accepted.

(Signatures of full team below)

X 

Name of team member: Hanna Hong

X 

Name of supervising teacher: Ji-Hoon Lee

Table of Contents

Abstract……1
Acknowledgements……...1
1. Introduction……...4
2. Experimental……5
2.1 Chemicals and materials……5
2.2 Conjugation of acridinium ester to Aβ42 aptamer……6
2.3 Temporary immobilization of the Aβ42 aptamer on the surface of graphene oxide (GO) film coated well……...6
2.4 Quantification of Aβ42……..7
2.5 Statistical analysis and determination of the LOD, LLOQ, accuracy, precision, and recovery of the aptasensor……...7
3. Results and Discussion……8
3.1 CL emission of Aβ42 aptamer-AE conjugate in AE chemiluminescence reaction……...8
3.2 Temporary immobilization of the Aβ42 Aptamer–AE conjugate on a GO film for Aptasensor development……..9
3.3 Optimization of experimental variables for the development of a sensitive Aβ42 Aptasensor…….……10
3.4 Optimization and Analytical Performance of the wash-free Aβ42 Aptasensor……...11
4. Conclusions……14
References……...15

1. Introduction

Over the past decade, the number of Americans living with Alzheimer's disease (AD) has continued to increase, largely because of population aging, although some studies have suggested a modest decline in age-specific dementia incidence.[1-2] Approximately 7.4 million Americans aged ≥65 years are living with Alzheimer's dementia in 2026.[3] At the same time, diagnosis is shifting from primarily symptom-based assessment toward earlier, biomarker-supported approaches using cerebrospinal fluid (CSF), positron emission tomography (PET), and, increasingly, blood-based biomarkers such as phosphorylated tau and amyloid-β (Aβ).[4-5]

Among the major biomarkers associated with AD, amyloid-β1–42 (Aβ42) plays a central role because a reduced concentration of Aβ42 in CSF is associated with its aggregation and deposition as amyloid plaques in the brain, one of the earliest pathological changes in AD.[6-7] Measurement of Aβ42, particularly together with Aβ40 and tau-related biomarkers, can therefore support the detection, classification, and monitoring of AD-related pathology before substantial cognitive decline occurs.[7-8]

Current analytical methods for Aβ42 rely predominantly on antibody-based immunoassays, particularly for CSF analysis.[9-10] Widely used automated platforms include electrochemiluminescence immunoassays, such as the Roche Elecsys β-Amyloid (1–42) CSF II assay, and chemiluminescent enzyme immunoassays, such as the Fujirebio LUMIPULSE system. These automated methods can provide results within tens of minutes and offer improved reproducibility and standardized operation.[11] Conventional ELISA and highly sensitive analytical methods such as mass spectrometry are also used, but they generally require longer processing times, more extensive sample handling, or specialized instrumentation.[12] In clinical applications, Aβ42 is increasingly interpreted together with Aβ40 as the Aβ42/Aβ40 ratio because normalization to Aβ40 can improve assessment of cerebral amyloid pathology compared with Aβ42 alone.[13]

Commercial ELISA kits remain widely used for quantitative determination of Aβ42 in research-use-only applications because of their established antibody-based specificity and standardized assay formats. However, conventional ELISA typically requires multiple incubation and washing steps, enzyme–substrate reactions, and repeated liquid-handling procedures, resulting in relatively long assay times. Consequently, aptasensors have been increasingly investigated as alternative platforms for Aβ42 detection.[14-17] Synthetic DNA or RNA aptamers offer several advantages, including chemical stability, reproducible synthesis, facile modification, relatively low production cost, and compatibility with diverse nanomaterials and signal-transduction technologies.[18-19]

Graphene oxide (GO) exhibits strong affinity for single-stranded DNA (ssDNA) and RNA through multiple noncovalent interactions, particularly π–π stacking between exposed nucleobases and the sp^2-hybridized aromatic domains of GO, together with hydrophobic interactions, hydrogen bonding, and electrostatic interactions.[20] Because the nucleobases of flexible single-stranded aptamers are readily accessible, ssDNA or RNA aptamers can adsorb efficiently onto the GO surface. In contrast, target-induced conformational changes and formation of aptamer–target complexes can reduce their affinity for GO and promote desorption.[20] These reversible interactions allow GO to function not only as a sensing interface but also as a temporary reservoir for aptamers, retaining and concentrating unbound aptamers on the surface until target binding promotes their release. Such a reservoir function can reduce the concentration of free signaling aptamers in solution, thereby lowering background signal and facilitating the development of simple wash-free or wash-minimized sensing formats.

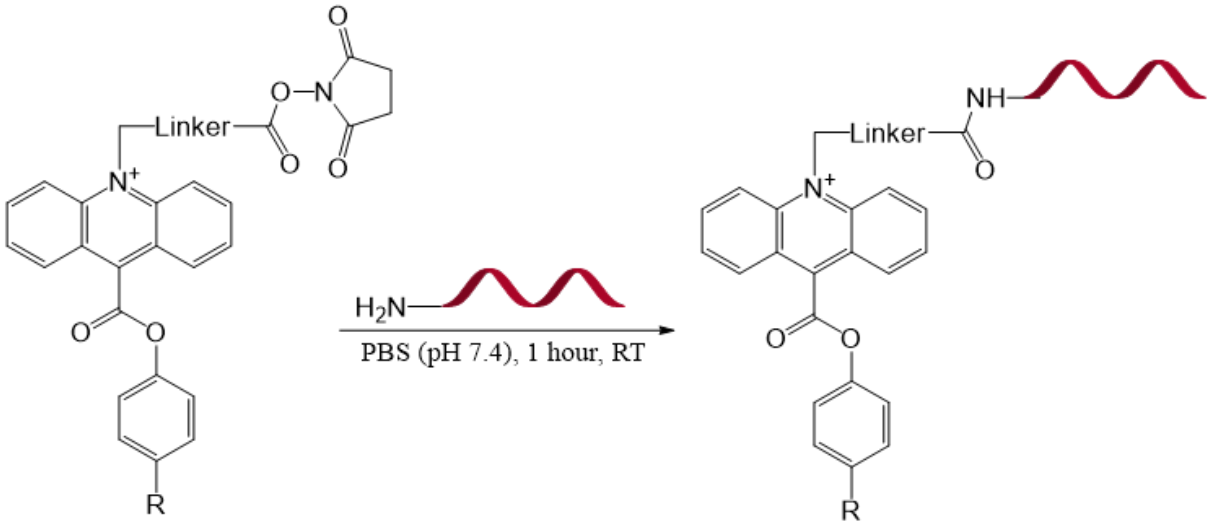
Based on the reversible adsorption of ssDNA aptamers onto GO, the high sensitivity of acridinium ester chemiluminescence (AE-CL), and the practical and economic advantages of synthetic aptamers, we hypothesized that GO could serve as a temporary reservoir for Aβ42 aptamer–AE conjugates, retaining unbound conjugates while allowing Aβ42-bound conjugates to be released into solution for chemiluminescence detection. Accordingly, the objective of this study was to develop a rapid, wash-free Aβ42 aptasensor by integrating GO-mediated aptamer immobilization and target-induced release with direct AE-CL detection. The analytical performance of the developed aptasensor was evaluated in terms of calibration characteristics, precision, recovery, specificity, and applicability to Aβ42 quantification, and its performance was compared with previously reported Aβ42 sensing methods.

2. Experimental

2.1 Chemicals and materials

The amine-conjugated Aβ42 aptamer (NH_2-C6-5′-GCCTGTGTTGGGGCGGGTGCG-3′), which has been widely used in the development of aptasensors,[21-23] was synthesized and supplied by Eurofins Genomics (Louisville, KY, USA). Acridinium NHS ester was purchased from AAT (Pleasanton, CA , USA). Aβ42, Aβ40, total tau antigens were purchased from BioLegend (San Diego, CA, USA). 3 and 30 % H_2O_2, 10 × PBS, 1N NaOH, and 1N HNO_3 were purchased from VWR (Radnor, PA, USA). Human serum albumin (HSA) and cetyltrimethylammonium chloride (CTAC) were obtained from Millipore Sigma (Rockville, MD, USA). Artificial cerebrospinal fluid (ACSF) A and B were purchased from Thomas Scientific (Swedesboro, NJ, USA). Bare wells coated with a graphene oxide (GO) film were provided by Luminescent MD (Hagerstown, MD, USA).

2.2 Conjugation of acridinium ester to Aβ42 aptamer



Scheme 1. Conjugation mechanism between acridinium NHS ester and the amine-modified Aβ42 aptamer.

The amine-conjugated Aβ42 aptamer was reacted with acridinium NHS ester at a 10-fold molar excess in 1× PBS (pH 7.4) containing 5% DMSO. The mixture was incubated at room temperature for 1hour protected from light. Free acridinium ester was subsequently removed using a 3-kDa molecular-weight-cutoff centrifugal filter. Scheme 1 illustrates the conjugation mechanism between acridinium NHS ester and the amine-modified Aβ42 aptamer.

2.3 Temporary immobilization of the Aβ42 aptamer on the surface of graphene oxide (GO) film coated well

50-µL aliquot of the Aβ42 aptamer–acridinium ester (AE) conjugate in PBS was added to a GO film-coated well to allow temporary immobilization through physical interactions between the aptamer and GO. After incubation for 30 minutes, unbound conjugate was removed by washing the well twice with PBS. The remaining unoccupied GO surface was blocked with 0.1% PVP for 2 minutes. The well was then washed twice with PBS, dried, and stored under ambient conditions until used to develop the Aβ42 aptasensor with acridinium ester chemiluminescence detection.

2.4 Quantification of Aβ42

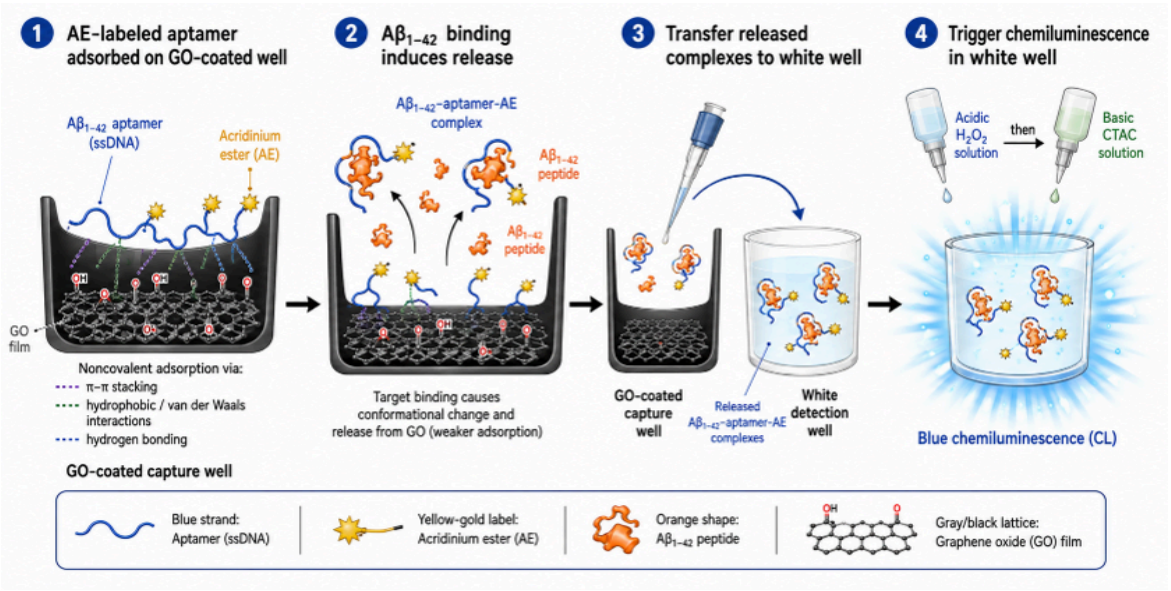


Figure 1. Aptasensor workflow for the quantification of Aβ42 using acridinium ester chemiluminescence detection.

As shown in Figure 1, 100 µL of an Aβ42 standard or sample was added to the aptasensor well containing temporarily immobilized Aβ42 aptamer–AE conjugates. The mixture was incubated for 30 minutes at room temperature (21 ± 2 °C) to allow Aβ42 to bind to the conjugates. After incubation, 40 µL of the solution containing the released Aβ42–aptamer–AE complexes was transferred to a borosilicate test tube. The tube was placed in an LB 9507 luminometer equipped with two syringe pumps (Berthold Technologies, Germany). The first pump injected 100 µL of acidic reagent containing 0.1 N HNO_3 and 0.5% H_2O_2. After incubation for 40 s, the second pump injected 100 µL of basic reagent containing 0.25 N NaOH and 7 mM CTAC, generating flash-type blue chemiluminescence. The relative chemiluminescence intensity was measured for 2 seconds.

2.5 Statistical analysis and determination of the LOD, LLOQ, accuracy, precision, and recovery of the aptasensor

Blank samples, Aβ42 standards, and spiked samples were analyzed in replication. Calibration curves were constructed by plotting relative chemiluminescence intensity against Aβ42 concentration and analyzed by regression. The limit of detection (LOD = B + 3S) was calculated as the mean blank signal (B) plus three standard deviations (S), whereas the preliminary limit of quantification (LLOQ = B + 10S) was calculated as the mean blank signal plus ten standard deviations and confirmed as the lowest concentration meeting the predefined accuracy and precision criteria. Accuracy was expressed as percent bias relative to the nominal concentration, precision as the coefficient of variation (CV), and recovery as the percentage of added Aβ42 recovered from spiked samples (N = 3).

3. Results and Discussion

3.1 CL emission of Aβ42 aptamer-AE conjugate in AE chemiluminescence reaction

Under alkaline conditions, hydrogen peroxide is converted to the hydroperoxide anion, which reacts with the acridinium ester label to form a high-energy dioxetanone intermediate. Rapid decomposition of this unstable intermediate produces electronically excited N-methylacridone. As the excited product returns to its ground state, blue chemiluminescence is emitted. CTAC enhances and stabilizes the light output, thereby improving detection sensitivity.

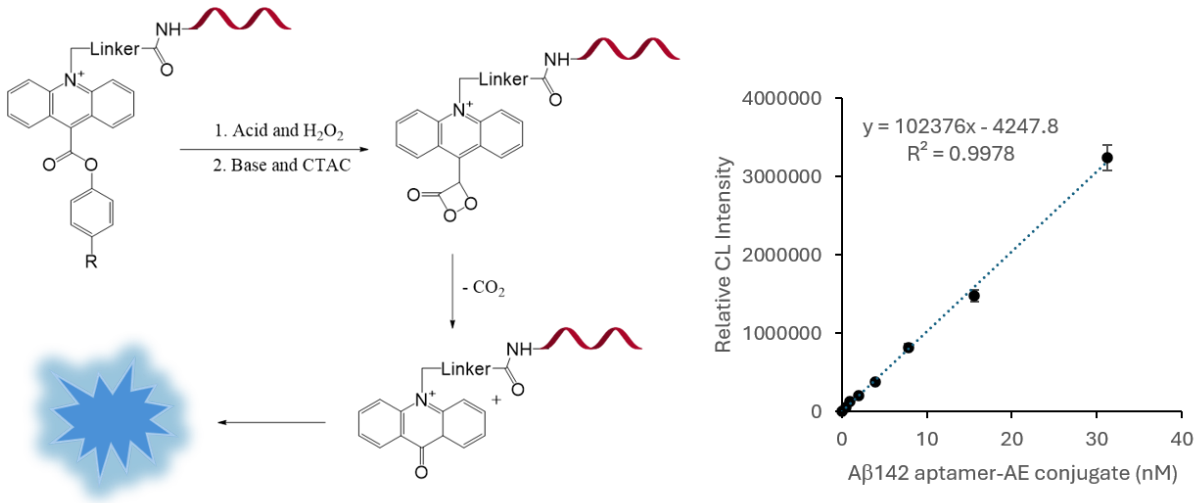


Figure 2. Acridinium ester chemiluminescence reaction mechanism and concentration-dependent relative CL intensity of the Aβ42 Aptamer–AE conjugate.

The relative chemiluminescence intensity increased linearly with the concentration of the Aβ42 aptamer–AE conjugate over the tested range. Linear regression produced the equation y= 102376x - 4247.8, with R^2 = 0.997, demonstrating a strong concentration-dependent response as shown in Figure 2. These results confirm successful AE conjugation and show that the conjugate generates a predictable chemiluminescence signal suitable for quantitative aptasensor development.

3.2 Temporary immobilization of the Aβ42 Aptamer–AE conjugate on a GO film for Aptasensor development

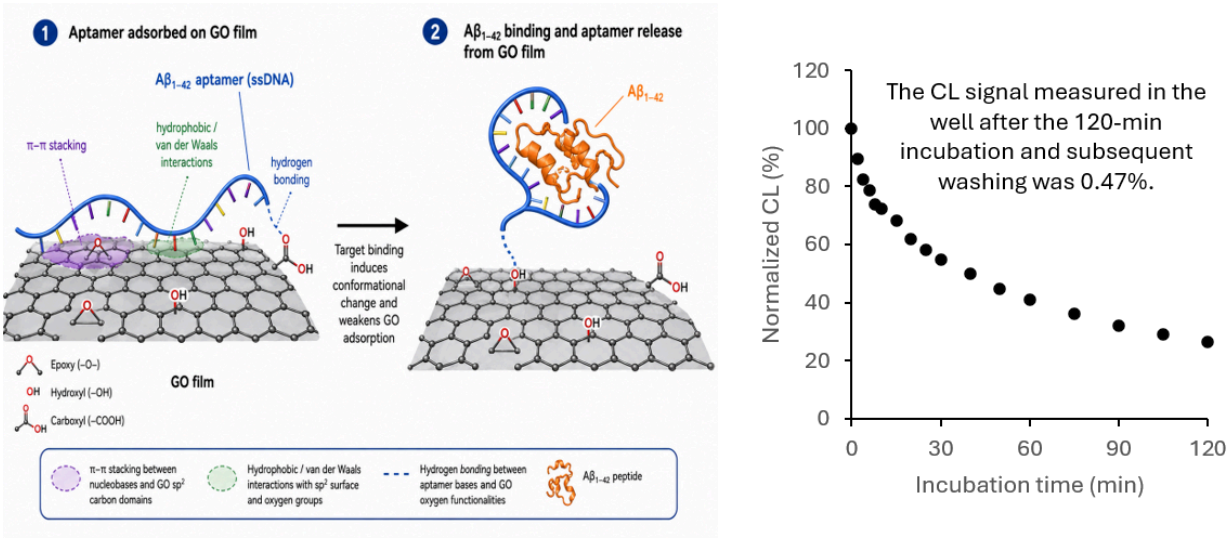


Figure 3. Mechanism of temporary Aβ42 Aptamer–AE conjugate immobilization on and Aβ42–Aptamer–AE complex release from the GO Film, with experimental verification of conjugate immobilization.

As shown in Figure 3, the Aβ42 aptamer–AE conjugate was temporarily immobilized on the GO film through noncovalent interactions. The exposed nucleobases of the aptamer interacted with the sp^2-carbon domains of GO through π–π stacking and hydrophobic/van der Waals interactions. Hydrogen bonding also occurred between the aptamer and the oxygen-containing functional groups on the GO surface. Upon binding to Aβ42, the aptamer underwent a conformational change that reduced its interaction with GO, resulting in the release of the Aβ42–aptamer–AE complex into solution. The AE label in the released complex subsequently generated a measurable chemiluminescence signal.

The graph shown in Figure 3 indicates that the normalized CL intensity of the conjugate remaining in solution decreased progressively with incubation time, from 100% initially to approximately 25% after 120 minutes. This decrease indicates time-dependent adsorption of the Aβ42 aptamer–AE conjugate onto the GO film. After washing, the residual CL signal attributable to unbound conjugates was only 0.47%, indicating that nearly all unbound conjugates were effectively removed. These results support the successful temporary immobilization of the Aβ42 aptamer–AE conjugate on the GO surface and its subsequent release following specific binding to Aβ42.

3.3 Optimization of experimental variables for the development of a sensitive Aβ42 Aptasensor

As shown in Figure 4A, increasing the volume of artificial CSF containing the Aβ42 aptamer–AE conjugate produced a progressive increase in relative CL intensity. The signal increased from approximately 5.0×10^4 at 10 µL to approximately 5.6×10^5 at 100 µL. This response was expected because a larger volume contained a greater amount of the AE-labeled conjugate available for chemiluminescence generation.

In contrast, the blank signal obtained using artificial CSF without the conjugate remained relatively constant, ranging from approximately 600 to 750 relative CL units over the tested volume range (Figure 4B). Thus, increasing the artificial CSF volume did not substantially increase the nonspecific background. Because the conjugate-associated signal increased while the blank remained stable, the S/B ratio increased markedly with volume, from approximately 70 at 10 µL to approximately 800 at 100 µL (Figure 4C). Based on these results, 100 µL was selected as the optimal sample volume because it generated the highest analytical signal, an S/B ratio.

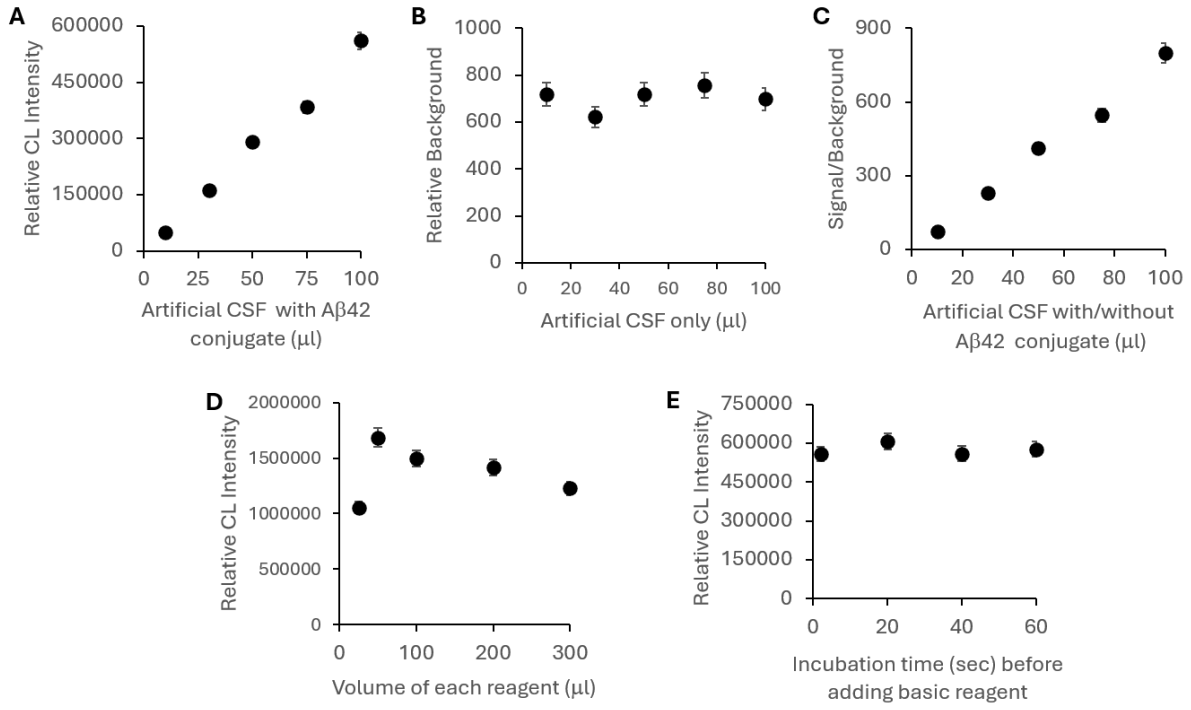


Figure 4. Optimization of experimental variables: (A) effect of the volume of artificial CSF containing the Aβ42 aptamer–AE conjugate; (B) effect of blank artificial CSF volume; (C) signal-to-background (S/B) ratio as a function of the volume of artificial CSF containing the Aβ42 aptamer–AE conjugate; (D) effect of equal volumes of the acidic and basic reagents; and (E) optimization of the incubation time after mixing the artificial CSF with the acidic reagent and before adding the basic reagent.

Figure 4D shows the effect of injecting equal volumes of the acidic and basic reagents. The CL intensity increased when the volume of each reagent was increased from 25 to 50 µL, reaching a maximum of approximately 1.7×10^6 relative CL units at 50 µL. Further increases in reagent volume gradually reduced the CL intensity. The lower signal at 25 µL may have resulted from insufficient reagent volume for efficient AE activation, whereas the decrease at larger volumes may have been caused by dilution of the AE-labeled conjugate or changes in the final reaction conditions. Therefore, 50 µL of each reagent produced the strongest CL response under the tested conditions.

The incubation time between the addition of the acidic reagent and the subsequent addition of the basic reagent was evaluated from 0 to 60 seconds (Figure 4E). The CL intensity remained relatively stable throughout this interval, ranging from approximately 5.5×10^5 to 6.0×10^5 relative CL units. The highest average signal was observed after approximately 20 seconds, although the differences among the tested incubation times were relatively small. An incubation time of 40 seconds was selected to provide sufficient time for the artificial CSF and acidic reagent containing H_2O_2 to equilibrate before the basic reagent was added to initiate flash-type chemiluminescence.

3.4 Optimization and Analytical Performance of the wash-free Aβ42 Aptasensor

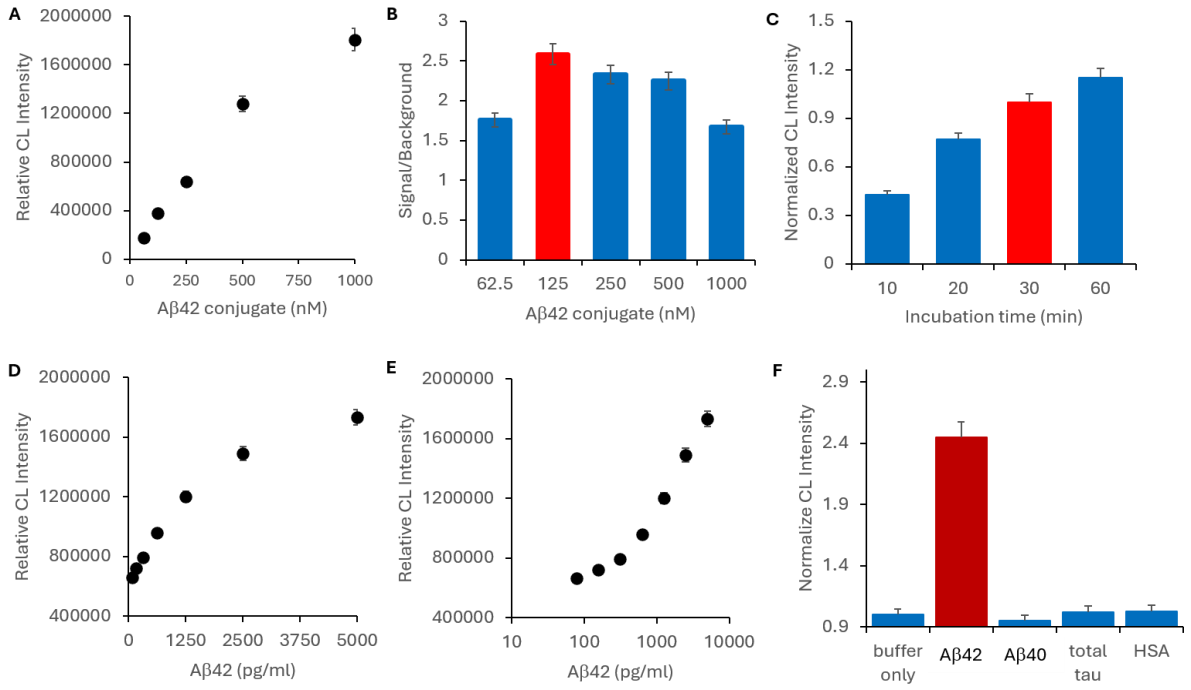


Figure 5. Optimization and analytical performance of the Aβ42 aptasensor: (A) effect of the Aβ42 aptamer–AE conjugate concentration used for temporary immobilization on the GO film-coated well; (B) signal-to-background (S/B) ratio as a function of the concentration of temporarily immobilized Aβ42 aptamer–AE conjugate; (C) effect of incubation time on the formation and release of the Aβ42–aptamer–AE complex; (D) calibration curve for Aβ42

concentrations ranging from 78.5 to 5,000 pg/mL; (E) calibration curve plotted against the logarithm of the Aβ42 concentration; and (F) selectivity of the Aβ42 aptasensor for Aβ42 compared with Aβ40, total tau, and human serum albumin (HSA).

The concentration of the Aβ42 aptamer–AE conjugate used for temporary immobilization on the GO film was first optimized. The CL intensity measured after immobilization and washing increased progressively as the conjugate concentration increased from 62.5 to 1,000 nM, indicating that greater amounts of the conjugate were retained on the GO surface (Figure A). However, the S/B ratio reached its maximum value of approximately 2.6 at 125 nM and subsequently decreased at higher concentrations (Figure B). The reduction in the S/B ratio at higher conjugate concentrations was likely caused by an increase in residual or nonspecific background relative to the target-dependent signal. Therefore, 125 nM was selected as the optimal conjugate concentration.

The normalized CL intensity increased with the Aβ42-binding incubation time, reaching approximately 0.43, 0.77, 1.00, and 1.15 after 10, 20, 30, and 60 minutes, respectively (Figure C). These results indicate that longer incubation allowed more Aβ42–aptamer–AE complexes to form and be released from the GO film. Although the signal continued to increase slightly up to 60 minutes, 30 minutes was selected as an appropriate compromise between assay sensitivity and analysis time. Under the optimized conditions, the relative CL intensity increased in a concentration-dependent manner over the Aβ42 range of 78.5–5,000 pg/mL (Figure D). The response increased rapidly at lower concentrations and more gradually at higher concentrations when plotted on a linear concentration scale. Plotting Aβ42 concentration on a logarithmic scale provided a useful calibration relationship across the entire tested range (Figure E). Based on the logarithmic calibration curve, the LOD and LLOQ were determined to be 27 and 78.5 pg/mL, respectively. The LLOQ corresponded to the lowest concentration quantitatively measured within the established calibration range.

The selectivity of the aptasensor was evaluated using Aβ42 and potentially interfering proteins, including Aβ40, total tau, and HSA (Figure F). Aβ42 produced a normalized CL intensity of approximately 2.45, whereas the buffer blank and interfering proteins generated normalized signals close to 1.0. Thus, the Aβ42 response was approximately 2.4-fold higher than the responses obtained from the blank and tested interfering proteins, demonstrating the preferential recognition of Aβ42 by the aptamer–AE conjugate. Selectivity was evaluated under stringent interference conditions using Aβ40 at 100 ng/mL, total tau at 2,500 pg/mL, and HSA at 0.2 mg/mL. The concentrations of Aβ40 and total tau exceeded their typical CSF ranges. Despite these high concentrations, all three potential interferents produced signals comparable to the buffer blank, whereas Aβ42 generated an approximately 2.4-fold higher response, supporting the high selectivity of the aptasensor.

The total analytical reaction and detection time was approximately 31 minutes, consisting of a 30-min antigen-binding step, a 40-s incubation with the acidic reagent, and a 2-s CL measurement. For comparison, the automated Roche Elecsys β-Amyloid (1–42) CSF assay requires approximately 18 minutes and has a reported LOD of 100–120 pg/mL and an LoQ of 150–200 pg/mL, depending on the cobas analyzer.[24] The aptasensor therefore exhibited an approximately 3.7–4.4-fold lower LOD and a 1.9–2.5-fold lower LLOQ than the Roche assay, although its analysis time was approximately 13 minutes longer. The Fujirebio Lumipulse G β-Amyloid 1–42 assay requires approximately 30 minutes, which is comparable to the aptasensor analysis time.[25] The FDA review reports an LOD of 11.6 pg/mL and an LoQ of 38 pg/mL for the Lumipulse assay.[26] Accordingly, the aptasensor's LOD and LLOQ were approximately 2.3- and 2.1-fold higher, respectively, than those of the Lumipulse assay.

Overall, the aptasensor provided greater analytical sensitivity than the Roche Elecsys assay and an analysis time comparable to that of the Lumipulse system. However, this comparison remains preliminary because the aptasensor was evaluated using artificial CSF, whereas the automated systems were extensively validated using human CSF under standardized clinical laboratory conditions. Direct analysis of identical human CSF samples will be necessary to establish comparative clinical performance.

Table 1. Recovery, accuracy, and precision of the Aβ42 Aptasensor in artificial CSF at three Aβ42 spike concentrations ($n = 3$).

Spiked sample	Spiked Aβ42 (pg/ml)	Measured Aβ42 (pg/ml)	Recovery (%)
1	200	184.5 ± 12.7	92.3
2	800	870.9 ± 36.5	108.9
3	1,500	1,690.5 ± 84.1	112.7

Recovery was evaluated at three Aβ42 concentrations using triplicate measurements (n=3). As shown in Table 1, The measured concentrations were 184.5±12.7, 870.9±36.5, and 1,690.5±84.1pg/mL for samples spiked with 200, 800, and 1,500 pg/mL Aβ42, respectively. The corresponding recoveries ranged from 92.3% to 112.7%, with a mean recovery of 104.6%, demonstrating acceptable accuracy across the tested concentration range. The coefficients of variation were 6.9%, 4.2%, and 5.0%, respectively, indicating good precision, with all CV values below 7%. A slight positive bias was observed at the two higher concentrations, particularly at 1,500 pg/mL, suggesting that further matrix-matched validation with additional replicates may be beneficial.

4. Conclusions

The GO-based Aβ42 aptasensor provided a concentration-dependent response over 78.5–5,000 pg/mL, with an LOD of 27 pg/mL and an LLOQ of 78.5 pg/mL within approximately 31 minutes. Recoveries of 92.3–112.7% and CVs below 7% demonstrated acceptable preliminary accuracy and precision. The substantially higher response to Aβ42 than to Aβ40, total tau, and HSA also supported the selectivity of the aptamer–AE conjugate.

Further studies should validate the assay using pooled and individual human CSF samples, larger sample numbers, additional interfering proteins, and multiple reagent lots and testing days. Optimization should also focus on shortening the 30-min binding step, improving recovery at higher concentrations, evaluating storage stability, and directly comparing the aptasensor with automated clinical systems using identical CSF samples. Development of a complementary Aβ40 assay could additionally enable determination of the clinically valuable Aβ42/Aβ40 ratio.

References

[1] Ge, J.; Ge, J.; Bao, M.; Zhang, L.; Li, K.; Ji, A.; Mao, X.; Jiang, X.; Yue, K.; Sun, J.; Luo, P., Epidemiological trends and cross-country inequalities in the global burden of Alzheimer's disease and other dementias in postmenopausal women from 1990 to 2021. Ageing Research Reviews 2026, 117, 103069.

[2] Serrano-Pozo, A.; Escott-Price, V.; Grinberg, L. T.; Pascoal, T.; Suárez-Calvet, M.; Dubois, B.; Sperling, R. A., Alzheimer's disease. The Lancet 2026, 407 (10544), 2241-2262.

[3] 2026 Alzheimer's disease facts and figures. Alzheimers Dement. 2026 Apr 21;22(4):e71345. doi: 10.1002/alz.71345. eCollection 2026 Apr.

[4] Yin, C.; Tang, X.; Zeng, J.; Wang, Z.; Mi, J.; Liang, Y.; Qin, D.; Feng, Q.; Wu, A., Next-generation biosensor technologies for Alzheimer’s disease: Innovations in diagnosis, monitoring, and treatment. Ageing Research Reviews 2026, 114, 102954.

[5] Ahamed, M. A.; Guo, B.; Khalid, M. A. U.; Pal, T.; Guo, F.; Guan, W., Point-of-care testing for early diagnosis and population screening of Alzheimer’s disease: Recent advances and perspectives. Nano Today 2026, 69, 103033.

[6] Ouyang, X.; Chia, R. S. L.; Chai, Y. L.; Chong, J. R.; Sim, M. A.; Jo, D.-G.; Arumugam, T. V.; Sethi, G.; Dawe, G. S.; Chen, C. P.; Lai, M. K. P., Peripheral biomarkers of neuroinflammation in Alzheimer’s disease and vascular dementia. Biochemical Pharmacology 2026, 250, 118077.

[7] Leuzy, A.; Mattsson‐Carlgren, N.; Palmqvist, S.; Janelidze, S.; Dage, J. L.; Hansson, O., Blood‐based biomarkers for Alzheimer's disease. EMBO Molecular Medicine 2021, 14 (1), EMMM202114408.

[8] Jack, C. R.; Bennett, D. A.; Blennow, K.; Carrillo, M. C.; Dunn, B.; Haeberlein, S. B.; Holtzman, D. M.; Jagust, W.; Jessen, F.; Karlawish, J.; Liu, E.; Molinuevo, J. L.; Montine, T.; Phelps, C.; Rankin, K. P.; Rowe, C. C.; Scheltens, P.; Siemers, E.; Snyder, H. M.; Sperling, R.; Elliott, C.; Masliah, E.; Ryan, L.; Silverberg, N., NIA-AA Research Framework: Toward a biological definition of Alzheimer's disease. Alzheimer's & Dementia 2018, 14 (4), 535-562.

[9] Bruggink, K. A.; Jongbloed, W.; Biemans, E. A. L. M.; Veerhuis, R.; Claassen, J. A. H. R.; Kuiperij, H. B.; Verbeek, M. M., Amyloid-β oligomer detection by ELISA in cerebrospinal fluid and brain tissue. Analytical Biochemistry 2013, 433 (2), 112-120.

[10] Hansson, O.; Zetterberg, H.; Vanmechelen, E.; Vanderstichele, H.; Andreasson, U.; Londos, E.; Wallin, A.; Minthon, L.; Blennow, K., Evaluation of plasma Aβ40 and Aβ42 as predictors of conversion to Alzheimer's disease in patients with mild cognitive impairment. Neurobiology of Aging 2010, 31 (3), 357-367.

[11] Chen, X.; Jiang, W.; Wang, L.; Han, B.; Yu, D.; Li, G.; Sun, J.; Liu, X.; Xie, Y.; Zhangx, G., Analytical validation and clinical performance of a chemiluminescence immunoassay panel for plasma biomarkers in Alzheimer's disease: a preliminary study. Clinica Chimica Acta 2026, 121300.

[12] Chang, H.; Kang, H.; Lee, S.-K.; Lim, J.; Kastanenka, K. V.; Kashiwagi, S.; Jun, B.-H., Plasmonic nanoplatforms for Alzheimer's disease biomarker detection: LSPR and SERS strategies toward clinical translation. Materials Today 2026, 98, 103428.

[13] Delaby, C.; Estellés, T.; Zhu, N.; Arranz, J.; Barroeta, I.; Carmona-Iragui, M.; Illán-Gala, I.; Santos-Santos, M. Á.; Altuna, M.; Sala, I.; Sánchez-Saudinós, M. B.; Videla, L.; Valldeneu, S.; Subirana, A.; Tondo, M.; Blanco-Vaca, F.; Lehmann, S.; Belbin, O.; Blesa, R.; Fortea, J.; Lleó, A.; Alcolea, D., The Aβ1–42/Aβ1–40 ratio in CSF is more strongly associated to tau markers and clinical progression than Aβ1–42 alone. Alzheimer's Research & Therapy 2022, 14 (1), 20.

[14] Zhang, J.; Zhao, Y.; Li, X.; Gu, M.; Xu, L.; Zhao, J.; Zhang, H., Rapid and simple separation and detection of Aβ42 in blood neuronal-derived extracellular vesicles using nanozyme-catalyzed colorimetric sensor. Talanta 2026, 296, 128439.

[15] Esparza, T. J.; Zhao, H.; Cirrito, J. R.; Cairns, N. J.; Bateman, R. J.; Holtzman, D. M.; Brody, D. L., Amyloid-beta oligomerization in Alzheimer dementia versus high-pathology controls. Annals of Neurology 2013, 73 (1), 104-119.

[16] Kim, J. A.; Kim, M.; Kang, S. M.; Lim, K. T.; Kim, T. S.; Kang, J. Y., Magnetic bead droplet immunoassay of oligomer amyloid β for the diagnosis of Alzheimer′s disease using micro-pillars to enhance the stability of the oil–water interface. Biosensors and Bioelectronics 2015, 67, 724-732.

[17] Wu, H.; Chai, C.; Islam, M. D. S.; Sheng, S.; Xie, G.; Chen, T., An aptamer-mediated EXPAR fluorescence biosensor for early and sensitive detection of Aβ42 and Aβ40. Analytica Chimica Acta 2026, 1406, 345513.

[18] Zhao, L.; Wang, P.; Qu, T.; Ji, Q.; Zhao, X.; Zhao, Y.; Chen, Y., Structure-guided strategies for aptamer screening and optimization: Advances and perspectives. TrAC Trends in Analytical Chemistry 2026, 201, 118870.

[19] Long, S.; Lyu, M.; Chan, C. H.; Chen, Z.; Lu, A.; Yu, Y., Antibodies and aptamers as affinity ligands for exosome isolation, detection, and targeted delivery: A review. International Journal of Biological Macromolecules 2026, 381, 154153.

[20] Pethe, A.; Priyadarshini, S.; Chamoli, S.; Tripathi, D.; Karki, K.; Khondekar, K. R.; Kumar, P., Graphene oxide-based DNA biosensing: Recent advances and emerging roles of artificial intelligence and machine learning. Microchemical Journal 2026, 222, 117219.

[21] Zhou, Y.; Lv, Y.; Dong, H.; Liu, L.; Mao, G.; Zhang, Y.; Xu, M., Ultrasensitive assay of amyloid-beta oligomers using Au-vertical graphene/carbon cloth electrode based on poly(thymine)-templated copper nanoparticles as probes. Sensors and Actuators B: Chemical 2021, 331, 129429.

[22] Lv, Y.; Zhou, Y.; Li, C.; Lv, C.; Dong, H.; Xu, M.; Zhang, J.; Yan, M., In situ formation of boronic acid-based covalent organic frameworks for specific and ultra-sensitive electrochemical assay of glycosylated amyloid-beta proteins. Talanta 2025, 285, 127435.

[23] Liang, X.; Yin, X.; Wang, H.; Meng, D.; Xu, R.; Meng, L.; Yang, Y., Aptamer-modified ratiometric fluorescent sensor based on metal-enhanced fluorescence for visual and portable detection of β-amyloid protein aggregates. Microchemical Journal 2026, 221, 116909.

[24] Roche Diagnostics, Intended use and measuring range of the Elecsys β-Amyloid (1-42) CSF II assay. 2026, https://diagnostics.roche.com/us/en/products/lab/elecsys-beta-amyloid-1-42-csf-ii-pid00000063.html

[25] Fujirebio Europe, Approximately 30-min analysis time for quantitative measurement of Aβ42 in human CSF. 2017, https://www.fujirebio.com/en/news-events/fujirebio-europe-launches-lumipulser-g-bamyloid-142-a-fully-automated-assay-aiding-in

[26] U.S. Food and Drug Administration, FDA-reviewed analytical performance, including an Aβ42 LOD of 11.6 pg/mL and LoQ of 38 pg/mL. 2022, https://www.accessdata.fda.gov/cdrh_docs/reviews/DEN200072.pdf